

Article

Complex Agent for Phosphate Sequestration from Digested Sludge Liquor: Performances and Economic Cost Analysis

Shi Yan ^{1,*}, Li Nie ^{1,*}, Juan Ren ², Wei Wang ^{3,4}, Jingtao Xu ⁵, Ning Wang ⁵  and Qian Zhao ^{5,*}

¹ School of Business Administration, Shandong University of Finance and Economics, Jinan 250014, China; 20053821@sdufe.edu.cn

² Jinan Urban Planning and Design Institute, Jinan 250001, China; renjuan379@126.com

³ Shandong Institute of Geological Sciences, Jinan 250013, China; veily91@163.com

⁴ Key Laboratory of Gold Mineralization Processes and Resources Utilization, Key Laboratory of Metallogenic-Geologic Processes and Comprehensive Utilization of Minerals Resources in Shandong Province, Jinan 250013, China

⁵ School of Municipal and Environmental Engineering, Shandong Jianzhu University, Jinan 250101, China; xujingtao@sdjzu.edu.cn (J.X.); wangning@sdjzu.edu.cn (N.W.)

* Correspondence: 20068472@sdufe.edu.cn (L.N.); zhaoqian@sdjzu.edu.cn (Q.Z.)

Abstract: Phosphorus (P) management in the “water-energy-resource-nexus” in wastewater treatment plants (WWTPs) remains a longstanding challenge. P adsorption from the P-enriched digested sludge liquor (DSL) is a comparatively more practical and economically viable approach for P recovery in WWTPs. However, high concentrations of impurities in DSL might pose a negative and interferential effect on P adsorption, hindering the application of sorbents or precipitation methods. Given such a situation, highly efficient and cost-effective sorbent towards P reclamation from DSL is highly needed. Therefore, this study aims to develop a novel complex agent containing aluminum coagulant and superparamagnetic nano-sorbent (SNS) that can be used in magnetic seeding coagulation for P recovery. The complex agents with different PACI: SNS ratios showed varied turbidity removal rates and P recovery efficiencies and the optimal ratio was 15 mg PACI: 15 g SNS. PAC and SNS showed significant interaction because PAC could enhance P adsorption by shielding the interferential effect of colloidal impurities. In addition, the complex is highly regenerative, with turbidity and P removal rate stably maintained at 70–80% after 10 adsorption/regeneration cycles. The cost-benefit analysis of the dosing complex agent showed a dosing cost of 0.154 EUR/m³, admittedly much higher than the conventional magnetic seeding coagulation, which could probably be covered by the profit if the expensive and rare P product is reclaimed. This work indicated that the complex agent was superior due to its high adsorption capacity, easy separation, and repeated dosing, and therefore had the potential for P recovery from DSL.

Keywords: phosphorus recovery; digested sludge liquor; magnetic seeding coagulation; superparamagnetic nano-sorbents; economic cost



Citation: Yan, S.; Nie, L.; Ren, J.; Wang, W.; Xu, J.; Wang, N.; Zhao, Q. Complex Agent for Phosphate Sequestration from Digested Sludge Liquor: Performances and Economic Cost Analysis. *Processes* **2023**, *11*, 2050. <https://doi.org/10.3390/pr11072050>

Academic Editor: Antoni Sánchez

Received: 7 June 2023

Revised: 4 July 2023

Accepted: 7 July 2023

Published: 9 July 2023



Copyright: © 2023 by the authors. Licensee MDPI, Basel, Switzerland. This article is an open access article distributed under the terms and conditions of the Creative Commons Attribution (CC BY) license (<https://creativecommons.org/licenses/by/4.0/>).

1. Introduction

Nowadays, phosphorus (P) resource management is like a missing piece of the puzzle in the “water-energy-resource-nexus” in wastewater treatment plants (WWTPs). P pollutants in the domestic wastewater, with total phosphorus (TP) of 5–15 mg/L and annually discharged amount of 3.78 million tons globally, have been generally recovered with low fraction [1,2]. More than 90% of phosphorus in sewage is channeled into waste bio-sludge discharged from the biological process, especially from the enhanced biological phosphorus removal-centered bio-treatment facilities, resulting in high loads of P-enriched sewage sludge for digestion, dewatering, and final disposal [3]. Indeed, most of the P in the sewage sludge would be released into the liquid phase again under anaerobic conditions in a digester, generating P-rich digested sludge liquor (DSL), the total phosphorus in

which was 87–478 mg/L at a pH of 4–5 [1]. It is more practical and economically viable to grasp P from the P-enriched sludge liquor than that from raw wastewater due to its large volume and low P concentration. As the WWTPs are undergoing a paradigm shift of treatment processes towards great environmental and economic sustainability, the current simple-removal philosophy for total phosphorus pollutants needs to be re-examined and P recovery addressed, especially considering the energy-intensive and water-consuming mining of phosphate rock [2].

The most viable option for P recovery is struvite (magnesium ammonium phosphate, $\text{MgNH}_4\text{PO}_4 \cdot 6\text{H}_2\text{O}$) or hydroxyapatite (CaP) crystallization. By adding Ca^{2+} and Mg^{2+} to the sludge liquor containing ammonia nitrogen and phosphate, struvite crystals formed and could be separated from the wastewater for later agricultural use as a slow-release fertilizer. The stable and effective Ca/struvite precipitation has been firmly established in Western European countries. In particular, many technologies, such as the DHV CrystalactorTM, Pelletiser FIX-Phosand P-RoC[®], etc., have gained success in the market [4–6]. Temperature-, Mg/P-, N/P-, and pH-controlling strategies are no easy tasks for optimal crystal formation and crystal growth. For instance, Guadie et al. found that the optimal conditions for forming struvite crystals were in neutral or slightly acidic environments, while there was almost no struvite crystal formation in phosphate once the pH value increased beyond 10.5 [7]. Aside from the P pollutants, DSL might also contain high concentrations of suspended solids (1000–2400 mg/L) [8]. Therefore, the large amount of organic matter in the sludge liquor might have an adverse effect on the crystallization process, producing low-quality P end-product.

Actually, the magnetic adsorption and separation method might be a “one stone two birds” strategy for P recovery from DSL. On one hand, the superparamagnetic nano-sorbent (SNS) developed based on the layered double hydroxide (LDH) or metallic oxides could provide a new idea for the rapid and efficient recovery of phosphate. SNS is composed of superparamagnetic nanomagnetic cores (Fe_3O_4 magnetite embedded in a porous SiO_2 matrix) and an LDH surface, which serves as the active phosphate adsorption center, while the Fe_3O_4 magnetic core serves as the carrier. SNS is easy to be separated from the liquid phase in a magnetic field. After being modified with various transitional metals, SNS could sequester P with high adsorption capacity [9–11]. Selectively, SNS has been found to exhibit high selectivity in the presence of competing ions due to the stronger complexation between phosphate and LDH loaded on SNS. In addition, SNS could be easily regenerated using NaOH or KOH. As revealed by Drenkova-Tuhtan et al., a high P removal rate (>90%) could be achieved even after 60 adsorption–desorption cycles [12]. On the other hand, magnetic particles combined with flocculation, i.e., the newly emerging magnetic seeding coagulation process attracting great attention for offering advantages of high turbidity removal, settleability improvement, and low energy consumption compared to the traditional coagulation process. The coagulants (polyamine chloride or polyferric chloride, PACl or PFC) mixed with magnetic seeds could remove more turbidities than the sole use of PACl. For example, the magnetic seeds could improve the aggregation and precipitation of nanoparticles from palm oil wastewater treatment, swine wastewater, textile wastewater, etc. [13–15]. Therefore, as for the treatment of P-enriched waste sludge, there is a need to rethink the management strategy of this coagulation process and to consider whether the seeds in the magnetic seeding coagulation process could be replaced with SNS. As such, magnetic coagulation and SNS adsorption have complementary advantages and can be combined or integrated, with phosphate being “recovered” rather than “removed”.

In recent years, comprehensive studies have been conducted for the synthesis of superparamagnetic P nano-sorbents. Nano-size core-shell Fe_3O_4 @LDHs composites with good super-paramagnetism were prepared by Yan et al., and the batch experiments results revealed an adsorption capacity of 36.9 mg/g by Fe_3O_4 @Zn-Al-LDH, with P recovered after 10 s separation from aqueous solution by introducing an external magnetic field [16]. Instead of LDH synthesis, the magnetic nanoparticles composed of zirconium-iron oxides were prepared and the P adsorption capacity could be enhanced with the decrease in Fe/Zr

molar ratios. This nano-sorbent showed high adsorption and strong selectivity toward phosphate with co-existing ions such as Cl^- , SO_4^{2-} , NO_3^- , etc., and the selectivity could be improved by doping transitional metals such as Zr, La, Se, or Hf [17,18]. Drenkova-Tuhtan et al. reported a pilot study of the reliability of superparamagnetic ZnFeZr nano-sorbent treating P-containing wastewater, with a P recovery rate of >90% and effluent phosphate concentration of <0.05 mg/L [3]. The novel magnetically recoverable magnetite/lanthanum hydroxides were also investigated for phosphate sequestration in a lake. However, the phosphate sorption efficiency could be significantly attenuated by 34–45% compared to that in water solution due to the interference from lake sediment substances [4]. Similarly, the impurities in sludge liquor might not only have an interferential effect on the P adsorption, but also result in the inactive adsorption sites during the sorbent regeneration. By now, little information is available for the integration of PACl and SNS and little research has been conducted for simultaneous SS removal and P recovery by dosing this type of complex agent. The role of PACl in the complex agent has not been investigated from the perspective of P recovery.

In this study, complex agents were prepared by combining aluminum coagulant (PACl) and SNS and used for P recovery from DSL. The novel agents were characterized in terms of P adsorption capacity, turbidity removal, and reusability. The coupling mechanism between PACl and SNS and the economic cost were also discussed. The specific objectives were to (1) prepare the complex agent and investigate the turbidity removal, P adsorption performances, and reusability; (2) investigate the effect of dissolved organic matter (DOM) in the DSL and elucidate the interaction mechanism between PACl and SNS in the complex agent; and (3) evaluate the economic cost of dosing the complex agent and make a comparison with the conventional magnetic seeding coagulation.

2. Materials and Methods

2.1. Complex Agent and DSL Characteristics

Complex agents were prepared by mixing PACl ($\text{AlCl}_3 \cdot 6\text{H}_2\text{O}$) and synthesized SNSs with different mass ratios. These super-paramagnetic nanoparticles were prepared using the co-precipitation method. Firstly, the $\text{Fe}_3\text{O}_4 @ \text{SiO}_2$ superparamagnetic nano or ultrafine particles were synthesized. Then, by calcination of Mg/Al LDH by dissolving $\text{MgCl}_2 \cdot \text{H}_2\text{O}$ and $\text{AlCl}_3 \cdot \text{H}_2\text{O}$ in a basic solution, La-LDH crystals were formed. Thereafter, the La-LDH was surface-modified by lanthanum-hydroxides loading with the pH maintained at 10. Finally, after crystalization in an 80 °C bath and washing with boiling deionized water and anhydrous ethanol repeatedly till the pH reached neutral, the MgAl-La-LDH loaded onto the $\text{Fe}_3\text{O}_4 @ \text{SiO}_2$ particles and SNSs were dried and finally harvested. The detailed procedures have been revealed by Zhao et al. [18]. Afterward, the surface configurations of the complex agent and SNSs were analyzed with a scanning electron microscope (SEM, ZEISS Gemini SUPRA55, Germany).

DSL was obtained from the lab-scale mesophilic digester (operating at 35 °C), which was fed with excess activated sludge in the WWTP treating domestic sewage in Shandong Jianzhu University. The detailed composition of DSL is shown in Table 1. Orthophosphate was the main component of the total dissolved P. In addition, according to ICP-AES analysis, the content of Zn was detected as 0.3~0.5 mg/L, while the concentration of other heavy metals, such as Cu, Pb, As, Cd, Cr, and Zn, was below the detecting limit.

Table 1. Typical water quality parameters or components of DSL.

Term	DSL
Total dissolved P (mg/L)	22.6 ± 1.4
Orthophosphate (mg/L)	20.3 ± 0.9
HCO ₃ ⁻ (mg CaCO ₃ /L)	57.2 ± 0.7
Cl ⁻ (mg/L)	47.6 ± 2.8
SO ₄ ²⁻ (mg/L)	5.2 ± 0.3
SS (mg/L)	135 ± 18
Zn ²⁺ (mg/L)	0.4 ± 0.1
Extracellular protein (mg/L)	20.5 ± 1.3
Polysaccharide (mg/L)	28.4 ± 0.7
pH	6.4 ± 0.2

Note: All the values in the table are written as “mean ± standard deviation”.

2.2. Adsorption and Clarification Batch Experiments

The complex agents, with PACl and SNS ingredients at different mass ratios (25 mg:5 g, 20 mg:10 g, 15 mg:15 g, 10 mg:25 g, and 5 mg:30 g), were respectively dosed into 5 jars containing 100 mL DSL at room temperature. These jars were capped and vigorously shaken in a shaker at 120 rpm for 12 h to reach saturation (pre-determined in the previous P adsorption-equilibrium test). Afterward, the supernatant was decanted through a magnet and filtered with a 0.45 µm filter, the TP concentration was determined according to the standard molybdenum blue method, and turbidity was assayed using a turbidimeter (HACH TU5200) [19]. The P removal performance was determined by calculating the ratio of the P loading amount (mg P/g) to the original P amount in DSL.

The adsorption capacity for phosphate at different equilibrium concentrations could be described by adsorption isotherms. The isotherm test was conducted by exposing 0.5–2.5 g dry mass of complex agent (with the PACl: SNS ratio as 15 mgPACl: 15 g SNS) to a 100 mL aqueous solution containing phosphate with a concentration of 20 mg P/L at room temperature. After 12 h agitation in a shaker at 120 rpm, q_e (mg/g), i.e., the amount of phosphate loaded per unit mass of the complex agent at the equilibrium, the maximum adsorption capacity can be determined. To fit the equilibrium data, Langmuir and Freundlich isotherm models were used, with equations defined as follows:

$$q_e = q_m K_L C_e / (1 + K_L C_e) \quad (1)$$

$$q_e = k_f C_e^{1/n} \quad (2)$$

in which C_e (mg/L) is the phosphate equilibrium concentration. k_f ((mg/g)/(mg/L)^{1/n}) and K_L (L/mg) are the Freundlich and Langmuir adsorption equilibrium constants, respectively. q_m represents the maximum adsorption capacity (mg/g). n is a constant indicating the Freundlich isotherm curvature. Each sample was assayed in triplicates. Results are shown as the means and standard deviations (error bars) of 3 replicates per point.

The extracellular protein and polysaccharide were determined by the Lowry method and anthrone colorimetry [20,21], respectively. The pH value was measured with a pH electrode (Leici PHS-25). Cl⁻ and SO₄²⁻ concentrations were quantified using IC (ICS-5000+, Thermo Scientific) (Jackson). All the assays were conducted in triplicate. The raw DSL-filtered samples before and after batch tests were also analyzed by the dimensional excitation-emission matrix (EEM) fluorescence technique using a fluorescence spectrophotometer (F-4500, Hitachi, Japan). An excitation range of 200–400 nm and an emission range of 220–550 nm were employed.

2.3. Desorption and Regeneration Experiments

P recovery rates and the reusability of the magnetic seeds, i.e., SNS in the complex agent, were tested within 10 treatment/reuse (adsorption/desorption) cycles. The desorption experiment, i.e., the PACl regeneration experiment in cycle 1, was conducted with

100 mL DSL dosed with a complex agent containing PACl and SNSs (15 mg:15 g). After 12 h agitation and 15 min sedimentation, 1 mL supernatant was taken to determine the turbidity and orthophosphate content, with P adsorption capacity (q_0) and turbidity removal rate calculated. The SNSs in the exhausted agent were separated with a magnet, rinsed with deionized water, and regenerated in 100 mL 2M NaOH solution for 12 h. 2M NaOH solution, as a generative agent, was prepared in advance, and OH^- in NaOH caused the outer-sphere complexation (phosphate and SNS) to proceed in converse, leading to new “adsorption sites” for phosphate in the next cycle of adsorption [11]. Then, the amount of phosphate in the supernatant (i.e., the desorption amount) was determined, with the P recovery rate calculated. Afterward, these SNSs were rinsed, dried, and mixed with 15 mg PACl before dosing into another 100 mL DSL. Thus, cycle 2 of adsorption started, with the P adsorption capacity in cycle 2 (q_1) being calculated. Therefore, the SNS regeneration efficiency in cycle 1 was determined by calculating the ratio of q_0/q_1 . Procedures were repeated in cycles 3–10, with ratios of q_i/q_0 calculated. The desorption and regeneration tests were performed in triplicate.

2.4. Chemicals

$\text{AlCl}_3 \cdot 6\text{H}_2\text{O}$, NaOH, $\text{FeCl}_3 \cdot 6\text{H}_2\text{O}$, $\text{FeSO}_4 \cdot 7\text{H}_2\text{O}$, NaHCO_3 , and lanthanum oxides were purchased from the Sinopharm Chemical Reagent Co., Ltd. (Beijing, China). Ethanol ($\text{CH}_3\text{CH}_2\text{OH}$), hydrochloric acid (HCl), anthrone, and chemicals used in the Lowry method were purchased from Aladdin (Shanghai, China).

2.5. Method of Calculation on Dosing Cost

The cost of dosing commercial magnetic powder and coagulants should be the product of dosage and the market uni-price. For SNS dosing, the cost should be the product of dosage and the manufacturing cost (sum of the reagents involved and the main expensive processing). As for complex agents, the cost should be calculated as the sum of the cost of SNSs and coagulant dosage. Lost amounts, especially for magnetic sorbents, should also be taken into account.

3. Results

3.1. Structural Characterizations of the Complex Agent

The SEM pattern of the complex agent and SNS are presented in Figure 1a,b, respectively. Both the complex agent and SNS composites had relatively regular shapes and smooth surfaces, without any noticeable difference between them. This could be explained by the dominantly high content of SNS in the complex agent. Maybe the complex agent showed seemingly little pores, which was probably due to the presence of powdered PACl. The complex agent for both bare SNS and the complex agent showed unclear core-shell structure, with a diameter ranging from 10 to 50 nm.

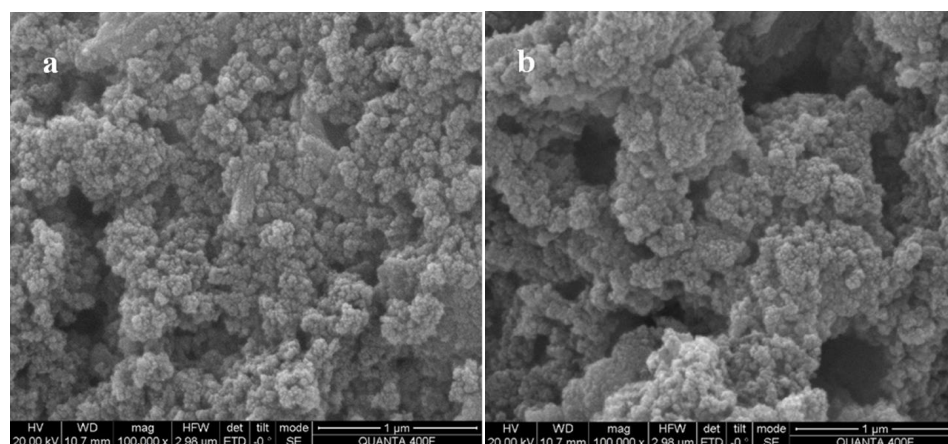


Figure 1. SEM image of (a) complex agent and (b) SNS.

3.2. TP and Turbidity Removal Performance by Complex Agent

Figure 2 exhibits the effect of the ratio of PACl and SNS mass in the mixtures on the turbidity removal rate and TP recovery efficiency. The turbidity removal performance varied with the PACl: SNS ratio in the dosed mixtures, with removal rates of 82.4%, 90.4%, 93.5%, 77.3%, and 70.2% after dosing 25 mg:5 g, 20 mg:10 g, 15 mg:15 g, 10 mg:25 g, and 5 mg:30 g of PACl: SNS, respectively. A dramatic decrease in removal efficiency was observed when dosing less than 10 mg/L of PACl, while, comparatively, more turbidities were removed when dosing >15 mg/L of PACl in the presence of PACl. 15 mg:15 g achieved the highest turbidity removal efficiency, because, at those dosages, the PACl played the primary role in the coagulation of colloidal or solid matter, while the SNS served as the magnetic seeds which benefited floc aggregation and precipitation. This result was consistent with the results reported by Lv et al. [22], who believed that the applied magnetic field could achieve effective sedimentation of the looser flocs and less production of fragments compared to the sole coagulation process, therefore resulting in improved turbidity removal rate. A dramatic decrease in the turbidity removal efficiency was observed when dosing 5 and 10 mg/L of PACl, although the component SNS simultaneously dosed was >25 g. This could be explained by the relatively high concentration of flocs in DSL and low concentration of coagulant dosed, which resulted in fewer opportunities for particle collision, and finally a lower coagulation efficiency [23]. According to previous literature, magnetic nanomaterials could affect sludge properties and extracellular polymer behavior by aggregating colloids into large flocs and greatly improve the separation performance of sludge and water. As a result, magnetic nanomaterials combined with macroscopic magnetic fields could promote a sludge dewatering effect and provide a relatively clarified supernatant for P sequestration [24,25].

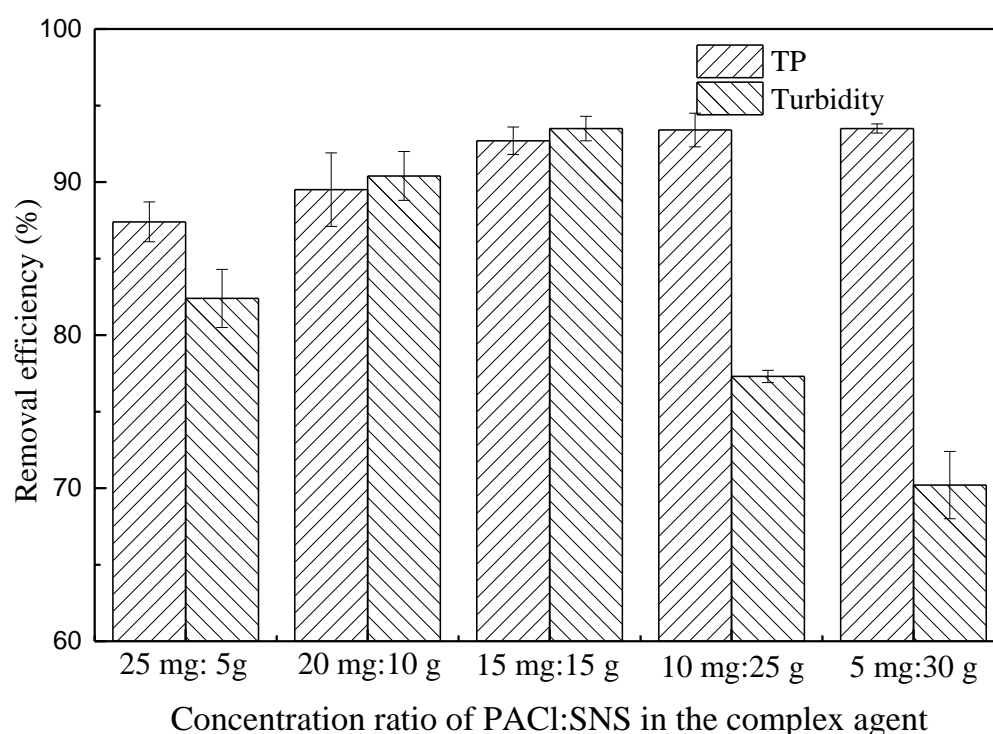


Figure 2. TP recovery and turbidity removal efficiency by complex agent-treating DSL.

As for the TP removal performance, the complex agent achieved removal efficiencies of >85% no matter how much the PACl and SNS ingredients were in the dosing mixtures. This could be explained by the similar P removal efficiency of PACl and SNS in spite of different mechanisms. PACl was precipitated with phosphorus while SNS grasped phosphorus by the means of adsorption or complexation reaction. After dosing the agent containing 15 mg

PACl and 15 g PACl, 93.5% of turbidity and phosphorus were simultaneously removed. During this process, The SNS particles instantly absorbed phosphate, and residual DOM and colloidal particles in the sludge liquor clustered with PACl, with the floc size increasing with the SNS particles as magnetic seeding.

Figure 3 presents the phosphate adsorption isotherm with complex agent/sole SNS plotted against different equilibrium P concentrations. The previous literature revealed that isotherm figures of P adsorption by SNS were more propitious to the Freundlich equation [11]. This tied well with the Freundlich-fitting curve in this study ($R^2 = 0.951$) in comparison with Langmuir-fitting results ($R^2 = 0.883$), which assumed multilayer covering is an adsorbent heterogeneous surface in which adsorption energy declined depending on the surface covering. However, the Freundlich model did not fit the data for the phosphate adsorption equilibrium experiment using the complex agent, with a coefficient of determination of $R^2 = 0.8653$. This explained the complicated P removal process driven by the complex agent. The P precipitation by the coagulant component and the P adsorption process by SNS could not be described by a pure adsorption model.

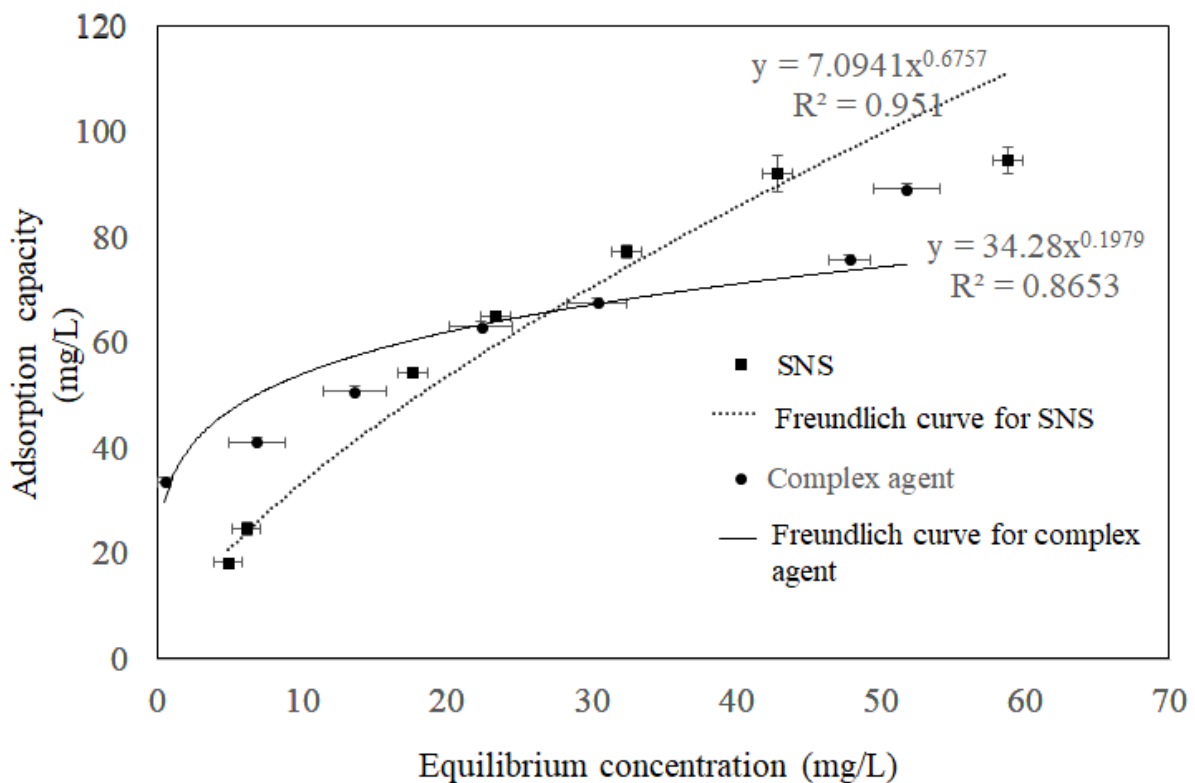


Figure 3. Phosphate adsorption isotherm with complex agent and sole SNS.

3.3. Reusability of Complex Agent

TP and turbidity removal performance by the complex agent during 10 cycles of treatment/reuse cycles is shown in Figure 4. The reusability test of SNS-PACl mixtures confirmed the effective recovery of SNS from flocs after applying a magnetic field, generating a 45% lower volume of particles compressed with PACl compared to that without SNS. During 10 cycles of SNSs recovery and PACl replenishment, the constantly stable turbidity removal performance was observed, with the removal percentage at the 10th cycle maintained at 70–80% of the original level in the 1st cycle. The DOC in the liquor followed similar patterns as turbidity, with concentration ranging from 814.8 mg/L to 903.2 mg/L. The relatively sharp reduction in turbidity removal rate after cycle 5 indicated that the 5th cycle might be the optimal cycle for this process. It was noteworthy that sole SNS without PACl also removed a small proportion of turbidity, which could be explained by the enmeshment and sweeping effect.

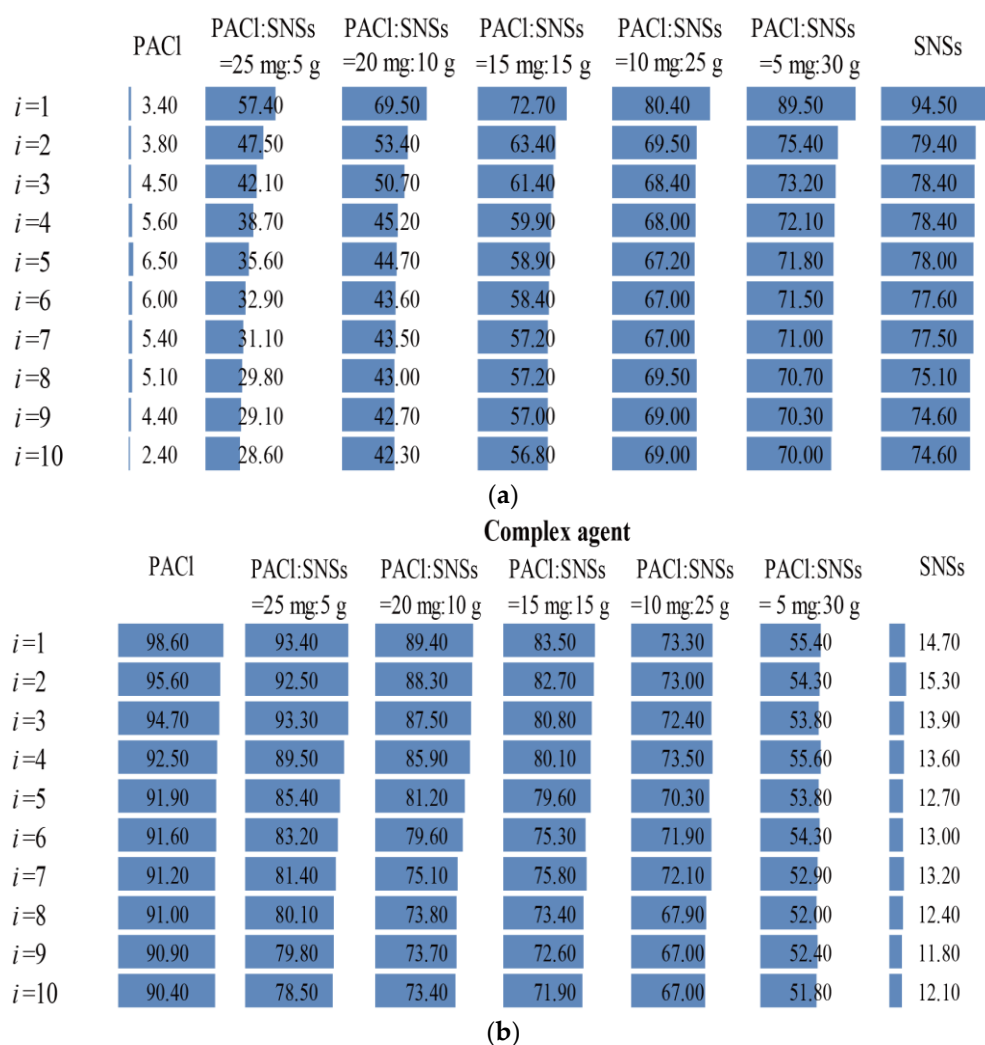


Figure 4. The variation of P (a) and turbidity (b) removal performance of complex agent during 10 cycles of treatment/reuse with complex agent.

During the treatment/reuse cycles, the P recovery amount was very low, indicating that the phosphorus removed by PACl could hardly be recovered. This small amount of P can be explained by the residual P as well as the P re-dissolved from the PACl flocs in the base solution during the regeneration process. In contrast, the P recovery performance was improved after the dosing of complex agents, with recovery efficiency increasing with the proportion of SNSs in the agent. The inner ligand complexation of phosphate with the LDH group on the surface of SNS, no matter in the form of H_2PO_4^- or HPO_4^- , has been considered a reversible reaction under alkaline conditions [11]. Though the P recovery rates dropped from 94.5% to 79.4% after the 1st cycle, they were maintained at 74.6–78.4% during the 2nd to 10th cycles. The complex agent with PACl: SNSs of 15 mg:15 g achieved a high recovery rate of both TP and turbidity (Figure 3). It also could be concluded that the phosphate preferred to be absorbed on SNS rather than precipitating with PACl because the inner complexation exhibited higher binding energy and stability. As such, it suggested mutually beneficial effects of the complexing agent containing SNS and PACl with a ratio of 1:3, because PACl removed all the impurities while SNS grasped the phosphate.

With the PACl-dominated complex agent, the P recovery rates decreased with regeneration cycles more dramatically than that with the SNS-dominated agent. It was presumably due to the deterioration of the coagulation effect caused by the caustic soda washing during regeneration. Though washed with deionized water, cycles of caustic regeneration might cause the pH value to fluctuate and reach 7.5 or above, under which

scenario the hydrolysate of the coagulant was mainly negatively charged and could not agglomerate through adsorption and electro-neutralization [26,27]. Limited amounts of PACl cannot facilitate the precipitate's enmeshment, leading to more P-adsorption interferential impurities, and therefore poorer P recovery performance.

3.4. Mechanism

Significant improvement in DOC removal (from 47% to 52%) was determined for the samples that were dosed with PACl-dominated complexing agents. The EEM spectra showed peak A at Ex/Em of 275/290–320 nm (Figure 5), indicating the presence of soluble microbial by-product-like substances for all the samples, while peak B at 350/430 nm (humic acid-like substances related to hydrophobic acids) was observed exclusively for the raw sludge liquor. These peaks were often found in the EEM spectra of bio-sludge EPS [28]. The hydrophobic acids could be almost completely removed by the sole SNS, while the PACl ingredient in the complexed agent removed the soluble microbial by-product-like substances, with removal efficiencies increasing with the content of PACl. This was consistent with the DOC removal performance and P recovery rates shown in Section 3.1, suggesting that PACl removed most of the potential P-adsorption-competing matter, i.e., probably the soluble microbial by-product-like substances. In addition, our previous study showed that SNS exhibited high selectivity towards phosphate in the presence of ions [29], but the hydrophobic PACl adsorbing to or absorbed on the SNS in this study might interfere with the phosphate adsorption. The addition of alum salts contributed to the removal of impurities, providing a comparatively simplified solution matrix for P adsorption.

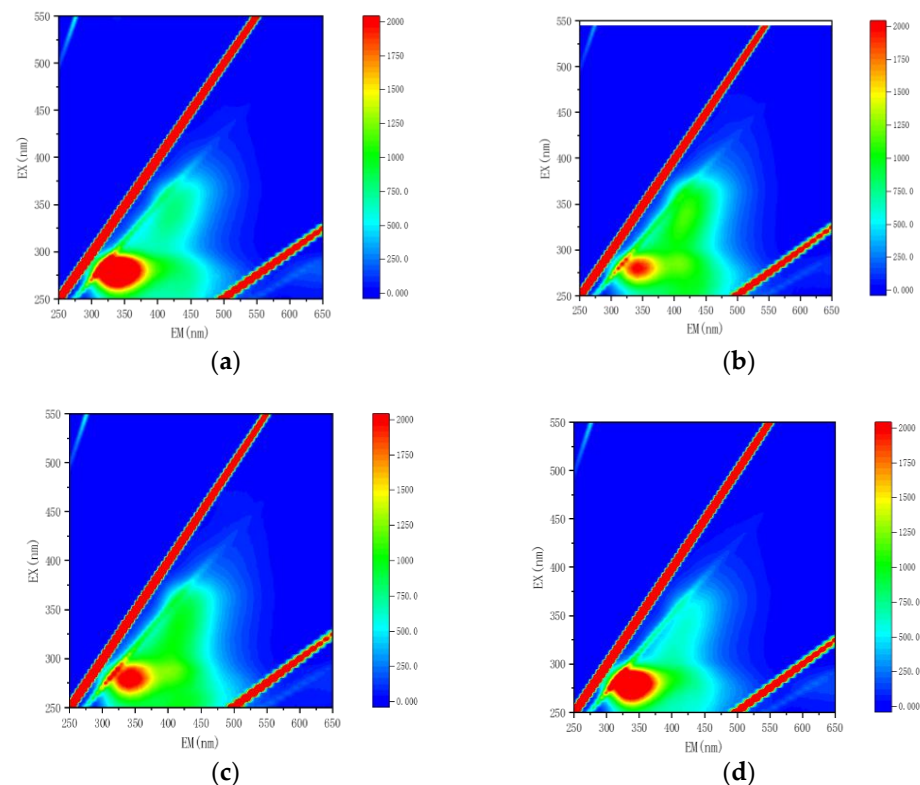


Figure 5. Profile of EEM for raw DSL (a) after treatment with complex agent containing PACl: SNS of 25 mg:5 g, (b) 15 mg:15 g, (c) and 5 mg:30 g (d).

It has been confirmed that SNS showed high selective capture ability and strong regeneration performance for phosphate even in the presence of coexisting ions such as nitrate, chloride ion, sulfate, etc. [10,18]. However, the LDH on the SNS surface exhibited strong affinity with the protein or soluble microbial by-product-like colloids in the DOM compo-

nents. As revealed by Gondim et al., human immunoglobulin G and serum albumin can be absorbed on the non-calcined Mg-Al LDH, and maximum IgG and HSA adsorption uptake occurred in phosphate buffer solution, suggesting that proteins and protein-like substances might interfere with the phosphate adsorption [30]. In addition, other biomacromolecules, including colloidal and soluble microbial products, and extracellular polymeric substances such as polysaccharides, short-chain fatty acids, nucleic acids, and humic acids might be also selectively adsorbed on the LDH-based sorbents, with “active sites” for phosphate decreasing. Once the cationic polymer PACI was added to the liquor, the negatively charged colloidal DOM would change from negative to almost neutral, and PACI cumulated into larger flocs (Figure 6), greatly assisting in the reduction of turbidity [31]. In addition, the induced PACI also acted as the nucleus to produce Al-DOM complexes. In the colloids-free solution, the SNS not only efficiently and rapidly adsorbed the phosphate ions, but also served as nuclei for aggregating by bridging these small aggregates into SNS-Al-DOM clusters, therefore reclaiming P, and meanwhile facilitating the clarification.

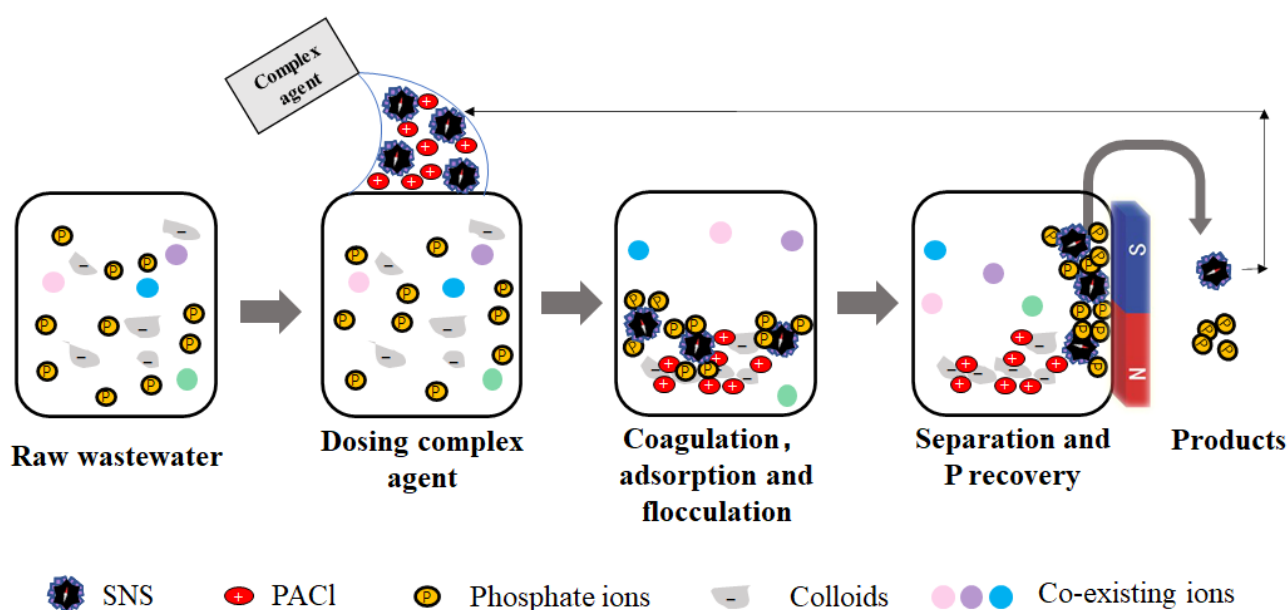


Figure 6. Coupling mechanism of PACI and SNS in the complex agent for P recovery from DSL.

3.5. Economic Analysis

Magnetic seeding coagulation has been regarded as cost-effective because inducing magnetic seeds in coagulation or clarified tank would promote the stable growth and rapid sedimentation of flocs, resulting in higher floc settling rate, faster settling velocity, shorter hydraulic retention, smaller tank size, and lower overall costs. It shows its necessity and feasibility for settling basins or facilities in cold areas where heating or insulation measures are required [32]. Our field investigation on the drinking water treatment plants in Weifang City revealed that 99% of magnetic seeds could be reclaimed, with the cost of the magnetic powder loss of only 0.00076–0.002 EUR/m³. Together with the cost of the coagulant dosing of 0.013 EUR/m³, the total cost of the conventional magnetic seeding coagulation was equivalent to about 0.015 EUR/m³, generating the clarified effluent containing TP of less than 0.05 mg/L, SS of less than 0.8 mg/L, and turbidity of less than 1NTU.

In this study, the magnetic seeds played a dual role in nucleating sites and P recovery. Based on the calculation of the previous test, the P adsorption capacity was in the range of 26.38–46.58 mg P/g SNS. An average of 24.9 g P could be produced after dosing 12.6 g SNS due to the decreasing adsorption capacity, i.e., the exhaustion of SNS after adsorption-regeneration cycles, with an agent synthesis cost of 0.14 EUR/g SNS. Considering the TP concentration of 20 g/m³ in the sludge liquor and SNS dosing amount of 10.12 g SNS/m³, 20 P could be reclaimed from 1 cubic liquor at a cost of the sole SNSs estimated to be

$10.12 \text{ g SNS/m}^3 \times 0.14 \text{ EUR/g SNS} = 1.4 \text{ EUR/m}^3$. Thus, the total dosing expense of the complex agent should be 0.14 EUR/m^3 (for PACL) + 1.4 EUR/m^3 (for SNS) = 1.54 EUR/m^3 , which could be extremely higher than the cost of the conventional magnetic seeding coagulation. The reclaimed crude P solution shows potential in producing phosphoric acid fertilizer or even some high-end industrial products such as glyphosate, glufosinate ammonium, or yellow phosphorus, which can compromise the high cost of SNS dosing. Considering the reclaimed 20 g/m^3 could be processed and produced as glufosinate ammonium ($\text{C}_5\text{HN}_2\text{O}_4\text{P}$, P of 15.6% in *w/w*) with a market price of 11,400 EUR/ton, the profit would be about $20 \text{ g/m}^3 \times 1 \text{ ton}/1,000,000 \text{ g} \div 15.6\% \times 11,400 \text{ EUR/ton} = 1.46 \text{ EUR/m}^3$, which could almost cover the cost of 0.154 EUR/m^3 due to the complex agent dosing. In addition, the environmental benefits would be more significant if taking into account PACL's role in avoiding eutrophication. The comparison of cost and environmental benefit between the magnetic seeding coagulation process and complex agent are shown in Table 2.

Table 2. Comparison of dosing cost and environmental benefit between magnetic seeding coagulation and complex agent.

	Magnetic Seeding Coagulation	Complex Agent
Cost (EUR/m ³)	0.015	1.54
Profit (EUR/m ³)	0	1.46
Net cost (EUR/m ³)	0.015	0.08
Environmental benefit	Low	High

4. Conclusions

This work investigated the performance of the complex agent consisting of PACL and SNS-treating DSL. The adsorption/clarification experiments demonstrated that both the turbidity removal and P recovery performance varied with the PACL: SNS ratio in the dosed agent, with PACL: SNS of 15 mg:15 g achieving the highest turbidity removal efficiency and comparatively high P recovery rate. In addition, constantly stable turbidity removal performance and regeneration efficiency could be maintained at 70–80% of the original level at the 10th cycle in the treatment/reuse (adsorption/desorption) batch tests. The 5th cycle might be the optimal cycle for this process using these materials because the turbidity removal rate dropped more significantly after cycle 5. The EEM profile indicated that induced Al species neutralized the negatively charged colloidal DOM, providing an almost interferences-free solution for the P recovery by SNS, while the SNS not only rapidly grasped the phosphate in large capacity, but also served as nuclei for the flocs aggregating by bridging these small aggregates into SNS-Al-DOM clusters. In spite of the high cost of SNS dosing, the economic cost calculation indicated that the complex agent would be promising if the reclaimed crude P solution can be processed and produced further for some high-end industrial products with higher added value after replacing the conventional magnetic seeding coagulation. It is expected that this study may foster further development and application of sustainable and efficient complex agents for P recovery from municipal wastewater or DSL with the ultimate aim of holistic water–energy–resource management in robust WWTPs.

Author Contributions: Conceptualization, S.Y., L.N. and Q.Z.; methodology, S.Y. and Q.Z.; software, J.X.; validation, W.W. and Q.Z.; formal analysis, N.W.; investigation, J.R. and W.W.; resources, J.R. and W.W.; writing—original draft preparation, S.Y., L.N. and Q.Z.; writing—review and editing, J.R., W.W., J.X. and N.W.; supervision, W.W. and J.R.; funding acquisition, L.N. and Q.Z. All authors have read and agreed to the published version of the manuscript.

Funding: This work was supported by the National Natural Science Foundation of China Project (grant number 51708338, 2017), Key Technology Research and Development Program of Shandong (2022CXGC021001), Shandong Province Natural Science Foundation (ZR2020ME228), Youth Innovation Technology Project of Higher School in Shandong Province (2019KJD003) and the Introduction

and Cultivation Plan for Young Innovative Talents of Colleges and Universities by the Education Department of Shandong Province.

Data Availability Statement: The data presented in this study are available on request from the corresponding author.

Acknowledgments: The authors would like to thank the School of Business Management at Shandong University of Finance and Economics and the key lab at the School of Municipal and Environmental Engineering, Shandong Jianzhu University.

Conflicts of Interest: The authors declare no conflict of interest.

Abbreviations

AAO	anaerobic–anoxic–oxic
DOM	dissolved organic matter
EEM	dimensional excitation-emission matrix
PFC	polyferric chloride
SNS	superparamagnetic nano-sorbent
WWTPs	wastewater treatment plants
CaP	hydroxyapatite
DSL	digested sludge liquor
PACl	polyaluminum chloride
P	phosphorus
TP	total phosphorus

References

- Bareha, Y.; Saoudi, M.; Santellani, A.-C.; Le Bihan, A.; Picard, S.; Mebarki, C.; Cunha, M.; Daumer, M.-L. Use of fermentation processes for improving the dissolution of phosphorus and its recovery from waste activated sludge. *Environ. Technol.* **2020**, *43*, 1307–1317. [[CrossRef](#)] [[PubMed](#)]
- Liu, Y.J.; Gu, J.; Liu, Y. Energy self-sufficient biological municipal wastewater reclamation: Present status, challenges and solutions forward. *Bioresour. Technol.* **2018**, *269*, 513–519. [[CrossRef](#)] [[PubMed](#)]
- Monea, M.C.; Löhr, D.K.; Meyer, C.; Preyl, V.; Xiao, J.; Steinmetz, H.; Schönberger, H.; Drenkova-Tuhtan, A. Comparing the leaching behavior of phosphorus, aluminum and iron from post-precipitated tertiary sludge and anaerobically digested sewage sludge aiming at phosphorus recovery. *J. Clean. Prod.* **2020**, *247*, 119129. [[CrossRef](#)]
- Fang, L.; Liu, R.; Li, J.; Xu, C.; Zhuang, L.; Wang, D. Magnetite/Lanthanum hydroxide for phosphate sequestration and recovery from lake and the attenuation effects of sediment particles. *Water Res.* **2018**, *130*, 243–254. [[CrossRef](#)]
- Li, B.; Boiarkina, I.; Yu, W.; Huang, H.M.; Munir, T.; Wang, G.Q.; Young, B.R. Phosphorous recovery through struvite crystallization: Challenges for future design. *Sci. Total Environ.* **2019**, *648*, 1244–1256. [[CrossRef](#)]
- Petzet, S.; Peplinski, B.; Cornel, P. On wet chemical phosphorus recovery from sewage sludge ash by acidic or alkaline leaching and an optimized combination of both. *Water Res.* **2012**, *46*, 3769–3780. [[CrossRef](#)] [[PubMed](#)]
- Guadie, A.; Belay, A.; Liu, W.; Yesigat, A.; Hao, X.; Wang, A. Rift Valley Lake as a potential magnesium source to recover phosphorus from urine. *Environ. Res.* **2020**, *184*, 10936. [[CrossRef](#)]
- Keefer, C.E.; Herman, K. Treatment of supernatant sludge liquor by coagulation and sedimentation. *Sew. Work. J.* **1940**, *12*, 738–744.
- Fang, K.; Peng, F.; Gong, H.; Zhang, H.; Wang, K. Ammonia removal from low-strength municipal wastewater by powdered resin combined with simultaneous recovery as struvite. *Front. Environ. Sci. Eng.* **2020**, *15*, 8. [[CrossRef](#)]
- Zhao, G.G.; Zhao, Q.; Jin, X.W.; Wang, H.B.; Zhang, K.F.; Li, M.; Wang, N.; Zhao, W.X.; Meng, S.J.; Mu, R.M. Preparation of a novel hafnium-loaded Fe₃O₄@SiO₂ superparamagnetic nanoparticles and its adsorption performance for phosphate in water. *Desalin. Water Treat.* **2021**, *216*, 188–198. [[CrossRef](#)]
- Zhao, Q.; Liu, C.F.; Song, H.Q.; Liu, Y.; Wang, H.B.; Tian, F.Y.; Meng, S.J.; Zhang, K.F.; Wang, N.; Mu, R.M.; et al. Mechanism of phosphate adsorption on superparamagnetic microparticles modified with transitional elements: Experimental observation and computational modelling. *Chemosphere* **2020**, *258*, 127327. [[CrossRef](#)]
- Drenkova-Tuhtan, A.; Schneider, M.; Franzreb, M.; Meyer, C.; Gellermann, C.; Sextl, G.; Mandel, K.; Steinmetz, H. Pilot-scale removal and recovery of dissolved phosphate from secondary wastewater effluents with reusable ZnFeZr adsorbent@Fe₃O₄/SiO₂ particles with magnetic harvesting. *Water Res.* **2017**, *109*, 77–87. [[CrossRef](#)]
- Chen, Y.; Sui, Q.; Yu, D.; Zheng, L.; Chen, M.; Ritigala, T.; Wei, Y. Development of a Short-Cut Combined Magnetic Coagulation-Sequence Batch Membrane Bioreactor for Swine Wastewater Treatment. *Membranes* **2021**, *11*, 83. [[CrossRef](#)] [[PubMed](#)]

14. dos Santos, T.R.T.; Mateus, G.A.P.; Silva, M.F.; Miyashiro, C.S.; Nishi, L.; de Andrade, M.B.; Fagundes-Klen, M.R.; Gomes, R.G.; Bergamasco, R. Evaluation of Magnetic Coagulant (α -Fe₂O₃-MO) and its reuse in textile wastewater treatment. *Water Air Soil Pollut.* **2018**, *229*, 92. [[CrossRef](#)]
15. Noor, M.H.M.; Azli, M.F.Z.M.; Ngadi, N.; Inuwa, I.M.; Opotu, L.A.; Mohamed, M. Optimization of sonication-assisted synthesis of magnetic *Moringa oleifera* as an efficient coagulant for palm oil wastewater treatment. *Environ. Technol. Innov.* **2022**, *25*, 102191. [[CrossRef](#)]
16. Yan, L.; Yang, K.; Shan, R.R.; Yan, T.; Wei, J.; Yu, S.J.; Yu, H.Q.; Du, B. Kinetic, isotherm and thermodynamic investigations of phosphate adsorption onto core-shell Fe₃O₄@LDHs composites with easy magnetic separation assistance. *J. Colloid. Interface Sci.* **2015**, *448*, 508–516. [[CrossRef](#)]
17. Zhang, C.; Li, Y.; Wang, F.; Yu, Z.; Wei, J.; Yang, Z.; Ma, C.; Li, Z.; Xu, Z.; Zeng, G. Performance of magnetic zirconium-iron oxide nanoparticle in the removal of phosphate from aqueous solution. *Appl. Surf. Sci.* **2017**, *396*, 1783–1792. [[CrossRef](#)]
18. Zhao, Q.; Tian, J.Z.; Zhang, K.F.; Wang, H.B.; Li, M.; Meng, S.J.; Mu, R.M.; Liu, L.; Yin, M.M.; Li, J.J.; et al. Phosphate recovery from the P-enriched brine of AnMBR-RO-IE treating municipal wastewater via an innovated phosphorus recovery batch reactor with nano-sorbents. *Chemosphere* **2021**, *284*, 131259. [[CrossRef](#)]
19. APHA. *Standard Methods for the Examination of Water and Wastewater*, 20th ed.; American Public Health Association: Washington, DC, USA, 1998.
20. Frølund, B.; Palmgren, R.; Keiding, K.; Nielsen, P.H. Extraction of extracellular polymers from activated sludge using a cation exchange resin. *Water Res.* **1996**, *30*, 1749–1758. [[CrossRef](#)]
21. Raunkjær, K.; Hvitved-Jacobsen, T.; Nielsen, P.H. Measurement of pools of protein, carbohydrate and lipid in domestic wastewater. *Water Res.* **1994**, *28*, 251–262. [[CrossRef](#)]
22. Lv, M.; Li, D.; Zhang, Z.; Logan, B.E.; van der Hoek, J.P.; Sun, M.; Chen, F.; Feng, Y. Magnetic seeding coagulation: Effect of Al species and magnetic particles on coagulation efficiency, residual Al, and floc properties. *Chemosphere* **2021**, *268*, 129363. [[CrossRef](#)]
23. Xue, Y.; Liu, Z.; Li, A.; Yang, H. Application of a green coagulant with PACl in efficient purification of turbid water and its mechanism study. *J. Environ. Sci.* **2019**, *81*, 168–180. [[CrossRef](#)]
24. Lakshmanan, R.; Rajarao, G.K. Effective water content reduction in sewage wastewater sludge using magnetic nanoparticles. *Bioresour. Technol.* **2014**, *153*, 333–339. [[CrossRef](#)] [[PubMed](#)]
25. Triques, C.C.; Fagundes-Klen, M.R.; Suzuki, P.Y.R.; Mateus, G.A.P.; Wernke, G.; Bergamasco, R.; Rodrigues, M.L.F. Influence evaluation of the functionalization of magnetic nanoparticles with a natural extract coagulant in the primary treatment of a dairy cleaning-in-place wastewater. *J. Clean. Prod.* **2020**, *243*, 118634. [[CrossRef](#)]
26. Meng, S.; Fan, W.; Li, X.; Liu, Y.; Liang, D.; Liu, X. Intermolecular interactions of polysaccharides in membrane fouling during microfiltration. *Water Res.* **2018**, *143*, 38–46. [[CrossRef](#)] [[PubMed](#)]
27. Meng, S.; Wang, R.; Zhang, K.; Meng, X.; Xue, W.; Liu, H.; Liang, D.; Zhao, Q.; Liu, Y. Transparent exopolymer particles (TEPs)-associated protobiofilm: A neglected contributor to biofouling during membrane filtration. *Front. Environ. Sci. Eng.* **2021**, *15*, 64. [[CrossRef](#)]
28. Li, K.; Qian, J.; Wang, J.F.; Wang, C.; Fan, X.L.; Lu, B.H.; Tian, X.; Jin, W.; He, X.X.; Guo, W.Z. Toxicity of three crystalline TiO₂ nanoparticles in activated sludge: Bacterial cell death modes differentially weaken sludge dewaterability. *Environ. Sci. Technol.* **2019**, *53*, 4542–4555. [[CrossRef](#)]
29. Hong, P.N.; Honda, R.; Noguchi, M.; Ito, T. Optimum selection of extraction methods of extracellular polymeric substances in activated sludge for effective extraction of the target components. *Biochem. Eng. J.* **2017**, *127*, 136–146. [[CrossRef](#)]
30. Gondim, D.R.; Cecilia, J.A.; Santos, S.O.; Rodrigues, T.N.B.; Aguiar, J.E.; Vilarrasa-Garcia, E.; Rodriguez-Castellon, E.; Azevedo, D.C.S.; Silva, I.J., Jr. Influence of buffer solutions in the adsorption of human serum proteins onto layered double hydroxide. *Int. J. Biol. Macromol.* **2018**, *106*, 396–409. [[CrossRef](#)]
31. Sabouhi, M.; Torabian, A.; Bozorg, A.; Mehrdadi, N. A novel convenient approach toward the fouling alleviation in membrane bioreactors using the combined methods of oxidation and coagulation. *J. Water Process Eng.* **2020**, *33*, 101018. [[CrossRef](#)]
32. Lapointe, M.; Barbeau, B. Selection of media for the design of ballasted flocculation processes. *Water Res.* **2018**, *147*, 25–32. [[CrossRef](#)] [[PubMed](#)]

Disclaimer/Publisher's Note: The statements, opinions and data contained in all publications are solely those of the individual author(s) and contributor(s) and not of MDPI and/or the editor(s). MDPI and/or the editor(s) disclaim responsibility for any injury to people or property resulting from any ideas, methods, instructions or products referred to in the content.